Magnetization steps near the irreversibility line in a mercury-based superconducting cuprate

V. Hardy, A. Daignère, and A. Maignan
Laboratoire Cristallographie et Sciences des Matériaux, Unité Mixte de Recherches 6508,
Institut des Sciences de la Matière et du Rayonnement et Université de Caen,
6 Boulevard du Maréchal Juin, 14050 Caen-Cedex, France
(Received 19 May 1999; revised manuscript received 15 September 1999)

Steps in the equilibrium magnetization curves of a $(Hg_{0.8}Cu_{0.2})Ba_2CuO_{4+\delta}$ (Hg-1201) single crystal have been detected in bulk magnetic measurements. The associated transition line in the H-T plane can be reasonably accounted for by melting or decoupling models, both leading to nearly the same value of the anisotropy parameter. The entropy changes along this line have been inferred from the height of the magnetization steps by assuming the underlying transition to be of first order. The order of magnitude of this entropy change, as well as its field and temperature dependences, is discussed in comparison to the available literature on other high-T_c superconductors.

I. INTRODUCTION

The existence of phase transitions in the vortex matter of high-T_c superconductors has recently attracted a lot of interest. Strong experimental evidence for a first-order transition, most often associated with vortex lattice melting, have been reported in $YBa_2Cu_3O_7$ (YBCO) (Refs. 1–7) and $Bi_2Sr_2CaCu_2O_8$ (Bi-2212).[8–14] For instance, very sharp jumps in local induction[8] have been detected by micro-Hall probe magnetometry in Bi-2212. In YBCO crystals, peaks in specific heat data[3–5] have also provided strong support for the occurrence of a first-order transition. Beside YBCO and Bi-2212, the existence of a vortex phase transformation has also been inferred from magnetization measurements in $(La_{1-x}Sr_x)CuO_4$ (Ref. 15) and in the organic superconductor κ-$(BEDT\text{-}TTF)_2Cu[N(CN)_2]Br$.[16,17]

In the frame of a first-order transition, the entropy variation at the transition can be directly derived from the jump in magnetization or the peak in specific heat. In most cases, the results are given in terms of entropy jump per vortex per superconducting layer, denoted Δs. It turns out that the temperature dependence of Δs is quite contrasted in the different compounds investigated so far: in YBCO, $\Delta s(T)$ is roughly constant in a large temperature range before dropping and extrapolating to zero a few kelvin below T_c;[2–4] in Bi-2212, Δs increases continuously with T and diverges approaching T_c;[8,12–14] in BEDT-TTF, Δs decreases almost linearly as T is increased and extrapolates to zero well below T_c.[16] A part of these discrepancies has been recently solved in the framework of the melting scenario.[18] In this study, Dodgson *et al.* have clearly pointed out the influence of the temperature dependence of the penetration depth, as well as the key role of the electronic anisotropy.

In this context, the investigation of a compound of intermediate anisotropy, having a T_c close to those of YBCO and Bi-2212, is strongly desirable. For this purpose, the mercury-based cuprate Hg-1201, possessing an electronic anisotropy close to 30 and an optimal T_c around 95 K,[19–21] is a well-suited candidate. The distance between adjacent CuO_2 planes is rather short in Hg-1201, namely, $d=0.95$ nm. According to estimates of the in-plane penetration depth ($\lambda_{ab}(0) \simeq 190$ nm) and of the anisotropy parameter ($\gamma \sim 30$), it turns out that the ratio $\lambda_{ab}(T)/\gamma d$ is always much larger than 1 for Hg-1201, in the whole temperature range. One thus deals with a layered compound in which Josephson coupling clearly dominates over electromagnetic coupling, in contrast to Bi-2212. This situation is also very different from the case of the more three-dimensional YBCO compound. The present paper reports on an experimental investigation of a first-order transition in Hg-1201.

II. EXPERIMENT

Single crystals of $(Hg_{0.8}Cu_{0.2})Ba_2CuO_{4+\delta}$ have been grown according to the method described in Ref. 21. The partial substitution of copper on the mercury sites was found to favor the growth of rather large crystalline specimens. The physical properties of these samples are roughly identical to those of all Hg-1201-type single crystals studied so far.[19,20] Their optimal T_c is close to 95 K, and their electronic anisotropy γ has been estimated to be close to 30.[21] Various superconducting properties of the present Hg-1201 single crystals have been previously studied[22] by magnetic measurements (irreversibility line, second-peak effect, in-plane penetration depth, superconducting fluctuations). Furthermore, the c-axis resistivity has been directly evaluated by transport measurements,[23] and the out-of-plane penetration depth λ_c has been inferred from magnetic imaging.[24]

The selected sample for the present study has approximate dimensions of $0.90\times0.85\times0.09$ mm^3, with the c axis along the thinnest direction. It is slightly underdoped with a T_c close to 92 K. It was pasted on the sample holder of the magnetometer with a tiny dot of silicon grease, in the geometry $H\|c$ axis. The transition width estimated from a shielding curve under 1 G is about 2.5 K.

The measurements were carried out by means of a (SQUID) superconducting quantum interference device magnetometer. Such a global technique unavoidably smooths the signatures of any transformation in the vortex matter, due to the inhomogeneity of internal field. Even in the reversible regime, a strongly nonuniform field distribution persists in a

platelet crystal.[25] It was shown, however, that the results obtained by SQUID magnetometry[10,14] and micro-Hall-sensors[8,12,13] in Bi-2212 are in good overall agreement about both the location of the transformation line and the derived values of entropy jumps.[26] Another problem with the standard measuring mode of a SQUID magnetometer is the inhomogeneity of the applied field along the scan length, which could yield spurious effects. At the same time, too short scan lengths can be detrimental to the quality of the signal fitting. As a compromise, we used a scan length of 2 cm, leading to a field variation smaller than 0.005% (e.g., 2 Oe under 40 000 Oe).

Measurements have been performed either as a function of field at fixed temperature or as a function of temperature at fixed applied field. The curves of magnetization versus applied field have been recorded for both increasing $[M_+(H)]$ and decreasing $[M_-(H)]$ field values. The equilibrium magnetization in the irreversible regime has been evaluated as $M_{eq} \simeq (M_+ + M_-)/2$. In a recent torque experiment on YBCO,[6] such an estimating procedure was demonstrated to yield reliable data. Measurements as a function of temperature under constant field have been registered in three different ways: standard zero-field-cooled $[M_{ZFC}(T)]$ and field-cooled-cooling $[M_{FCC}(T)]$ modes, as well as curves of thermoremanence $[M_{THR}(T)]$ measured upon warming after saturation of the magnetization at low temperature. Similarly to the case of $M_{\pm}(H)$, symmetrical profiles of the internal field are expected in $M_{ZFC}(T)$ and $M_{THR}(T)$, allowing us to estimate the equilibrium magnetization as $M_{eq} \simeq (M_{ZFC} + M_{THR})/2$. In all cases, the measurements at each value of H and T were recorded during 20 min. The first advantage of this procedure is an enlargement of the reversible regime due to magnetic relaxation. It also allows us to test the validity of the M_{eq} extrapolation in the irreversible regime by comparing the relaxation rates on both branches.

III. RESULTS

Figure 1 shows the high-field part of the hysteresis loop at $T=20$ K in a logarithmic field scale. The data presented here correspond to a waiting time of 20 min after each field change. It can be clearly seen that the magnetization curve in the reversible regime exhibits a smooth step between two fairly linear parts. In such a logarithmic scale, these linear regimes around the crossover can be fitted by parallel lines, allowing the step height to be simply defined as the shift between them. In the following, we will consider the knee on the high-field side as the characteristic field of the crossover (see Fig. 1). This characteristic field $H^*(T)$ lies within the reversible regime at all temperatures.

As T is increased, the low-field reversible domain below the step becomes less well defined. This is illustrated in the left part of Fig. 1, with the hysteresis loop at $T=25$ K, enlarged around the irreversibility field. One can observe that the ascending and descending branches first cross before merging. Let us refer this first crossing point to the standard notion of irreversibility fields, H_{irr}. There is a restricted range of fields above H_{irr} within which the two branches are slightly inverted. However, the hysteresis is so small in this case that one can safely estimate M_{eq} by averaging the

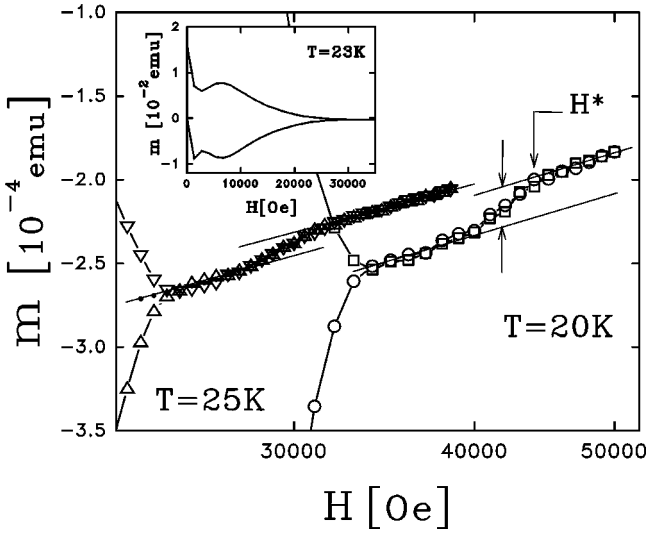

FIG. 1. Ascending (○) and descending (□) branches of a loop at $T=20$ K (corresponding to a waiting time of 20 min). Ascending (Δ) and descending (∇) branches of a loop at $T=25$ K (corresponding to a waiting time of 10 min). The solid circles are estimates of $M_{eq}(H)$ obtained by averaging both branches. Note that these data are plotted in a logarithmic field scale. At each temperature, the parallel lines are fits to the data on each side of the step. The shift between them yields the step height. The characteristic field $H^*(T)$ is associated with the *upper corner* of the step. The inset shows a complete half-loop at the intermediate temperature $T=23$ K.

$M_+(H)$ and $M_-(H)$ curves. These extrapolated M_{eq} values at $T=25$ K are plotted as solid circles in Fig. 1. As previously seen at lower temperatures, one observes a clear step connecting two field ranges which can be fairly fitted by parallel lines. Note that the magnitude of these magnetization steps is rather small. They are totally undetectable on the scale of a complete hysteresis loop, as illustrated in the inset of Fig. 1.

The occurrence of a magnetization step can also be investigated by measurements as a function of temperature. Figure 2 shows the $M_{ZFC}(T)$, $M_{FCC}(T)$ and $M_{THR}(T)$ curves under 3 T. One can observe that all three curves are well superimposed above 22 K. In this nearly reversible regime, one can clearly detect a kink on the magnetization curves. The inset shows an enlargement of the region under consideration. The solid lines correspond to the $M_{ZFC}(T)$ and $M_{THR}(T)$ curves. These curves actually cross at 22 K, and they are thus slightly inverted over a few kelvins in this nearly reversible regime, similarly to what occurs with $M_+(H)$ and $M_-(H)$ in Fig. 1, at $T=25$ K. The residual hysteresis is still very small in these T scans, and both curves exhibit exactly the same shape in the crossover region. One can therefore consider the averaged data of $M_{ZFC}(T)$ and $M_{THR}(T)$ as a fair estimate of $M_{eq}(T)$ (solid circles in the inset of Fig. 2). It can be noted in Fig. 2 that M_{FCC} tends to slightly increase as the temperature is decreased, demonstrating that these measurements cannot be used to estimate $M_{eq}(T)$ in the irreversible regime. As shown in the inset, one can determine a characteristic temperature T^* and the associated step height, similarly to what is done in the case of H scans. It must be emphasized that the results of the H scans in Fig. 1 (at T

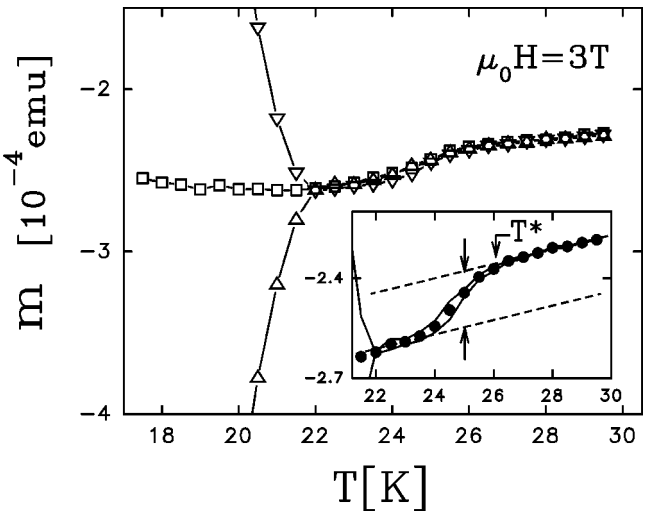

FIG. 2. Zero-field-cooled (Δ), field-cooled-cooling (□), and thermoremanent (∇) curves under 3 T. These data correspond to a waiting time of 10 min. The inset is an enlargement around the closing point, displaying the $M_{ZFC}(T)$ and $M_{THR}(T)$ curves (solid lines), together with the averaged data (●). The characteristic temperature $T^*(H)$ is defined similarly to $H^*(T)$. A linear temperature scale is used to derive the step height from the shift between parallel lines fitting to the data on each side of the step.

=25 K) and the T scans of Fig. 2 (under 3 T) are very well consistent about both the location and the height of the step.

Let us now focus on the measurements as a function of field. One observes that the problems encountered at 25 K become more and more pronounced as T is increased. Figure 3 displays enlargements of hysteresis loops at 40 K in the closing region, for different values of the waiting time, t_w, following each field change: 1 min, 4 min, and 20 min. The huge effect of magnetic relaxation is patent in the low-field side of Fig. 3. One also observes that the inversion between the $M_+(H)$ and $M_-(H)$ curves above H_{irr} becomes more marked as t_w increases. The hysteresis loop at $t_w=20$ min displays a *bubblelike* feature just above H_{irr} which is clearly

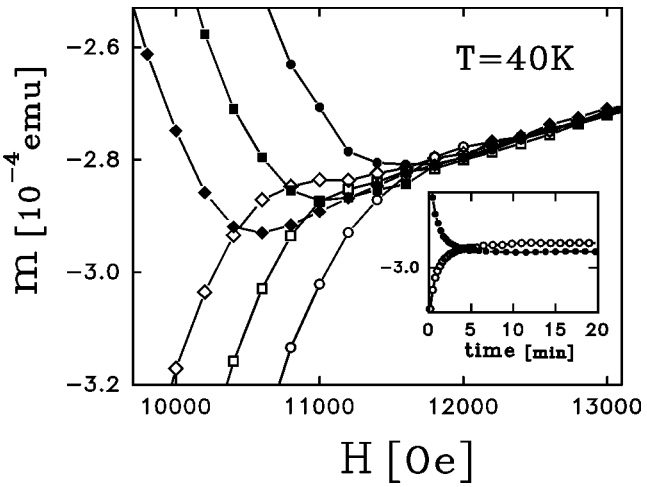

FIG. 3. Ascending (open symbols) and descending (solid symbols) branches of loops at $T=40$ K, corresponding to waiting times of 1 min (circles), 4 min (squares), and 20 min (diamonds). The inset shows the magnetic relaxation on the ascending (○) and descending (●) branches, under 11 000 Oe.

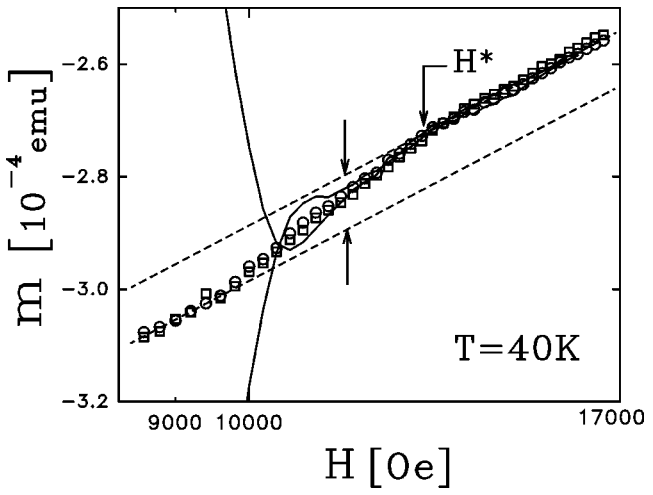

FIG. 4. The solid lines are the ascending and descending branches of the loop at $T=40$ K, for a waiting time $t_w=20$ min. The symbols are estimates of $M_{eq}(H)$ inferred from averaging the branches, at two values of t_w: 4 min (□) and 20 min (○).

wider than at shorter times. The inset shows that, in this field range, the relaxation curves on both branches actually exhibit a crossing in time. These relaxation curves also indicate that the shift in magnetization between both branches tends to become constant at long times. One can note that the development of similar a ''anomalous hysteresis'' as T is increased has previously been reported in the case of Bi-2212.[11] The shape of the SQUID responses has been checked to be satisfying for signal processing over the whole field range.

Figure 4 displays the calculated $M_{eq}=(M_+ + M_-)/2$, for two characteristic times ($t_w=4$ and 20 min), together with the M_+ and M_- curves at $t_w=20$ min. It turns out that both $M_{eq}(H)$ curves are nearly superimposed, demonstrating that the relaxation rates on both branches of the loop are very well symmetric. The observation of such behavior was used as a basic requirement to take the extrapolated M_{eq} values into account. With these data, one can observe in Fig. 4 a step in magnetization resembling those found at lower temperatures. The step height is still associated with the shift in magnetization between the logarithmic regimes at low and high fields. At 45 K, the step height is found to be noticeably decreased. For $T \geqslant 50$ K, there is no longer any clear indication of a step in magnetization. Within the experimental uncertainty, any M_{eq}-vs-ln(H) curve in this T range actually appears as a simple straight line over a wide field domain around H_{irr}.

Figure 5 displays the characteristic line in the H-T plane, which is associated with the occurrence of magnetization steps. Since the magnetization is much smaller than the applied field along this line, the magnetic induction B^* can be fairly approximated by H^*. We have reported both the $B^*(T)$ and $T^*(B)$ values extracted from the H and T scans, respectively. There is clear agreement between both sets of data. These kinks on equilibrium magnetization curves can be associated with a phase transition in the vortex state. The most often proposed transitions are melting of a flux-line lattice or decoupling of a flux-line liquid (a concomitant occurrence of both phenomena, leading effectively to sublimation, has also been evoked). As already specified, the c-axis

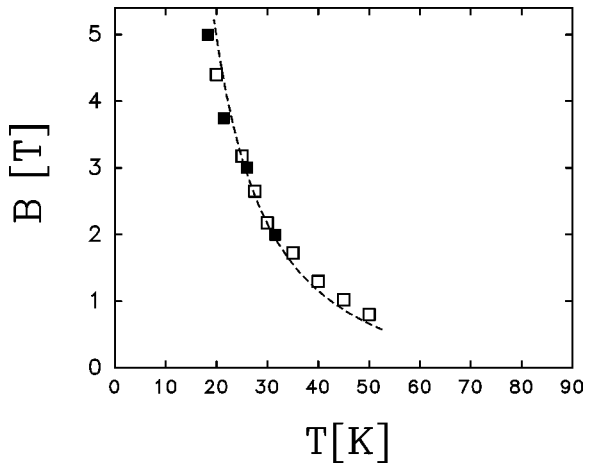

FIG. 5. Characteristic fields $H^*(T)$ derived from H scans (□) and characteristic temperatures $T^*(H)$ derived from T scans (■). The dashed line is a fit to the data with Eq. (3.1), corresponding to the melting transition.

coupling in Hg-1201 is predominantly of Josephson nature. We thus have to consider proper forms of the theoretical expressions for each of these characteristic fields.[27] The melting field[28,29] B_{m} and the decoupling field[27,30,31] B_{d} are expected to be of the form

$$B_{\mathrm{m}}=\frac{\alpha_m}{64\pi^3}\,\frac{c_L^4\Phi_0^5}{\gamma^2\lambda_{ab}^4 k_{\mathrm{B}}^2 T^2}, \tag{3.1}$$

$$B_{\mathrm{d}}=\frac{\alpha_d}{16\pi^2}\,\frac{\Phi_0^3}{\gamma^2 d\lambda_{ab}^2 k_{\mathrm{B}} T}, \tag{3.2}$$

where Φ_0 is the flux quantum, k_{B} is the Boltzmann constant, c_L is the Lindemann constant, d is the interdistance between CuO_2 planes, λ_{ab} is the in-plane penetration depth, γ is the electronic anisotropy, $\alpha_d \simeq (\pi e)^{-1} \simeq 0.1$, and α_m is a correcting factor of the order of unity. According to Ref. 29, $\alpha_m \sim \ln(B_{c2}/B)/8$. The T dependence of λ_{ab} can be written in the form $\lambda_{ab}(T)=\lambda_{ab}(0)/\sqrt{1-t^n}$, where t is the reduced temperature ($t=T/T_c$), and n has a value ranging between $n=1$ (Ginzburg-Landau behavior) and $n=4$ (two-fluid behavior). The dashed line in Fig. 5 corresponds to the best fit to the data with Eq. (3.1) corresponding to the melting model (with $n=4$ and $T_c=92$ K). Note that the somewhat arbitrary identification of H^* to the highest field of the crossover could contribute to the rather poor quality of this fit. Considering $\lambda_{ab}(0) \simeq 190$ nm,[22] $c_L \simeq 0.15$, and $B_{c2}/B \simeq 50$, one obtains $\gamma \simeq 31$. An equally good fit can be obtained within the frame of the decoupling model (with $n=1$ and $T_c=90$ K).[32] One derives from Eq. (3.2) a value of the anisotropy parameter, $\gamma \simeq 34$, which is very close to the previous one. It must be emphasized that these estimates are very well consistent with previous results ($\gamma \sim 30$) obtained from direct investigations by angular measurements.[19,20]

Figure 6(a) shows the temperature dependence of the step height at the transition. The alternative representation as a function of field is given in the inset. The error bars correspond to the uncertainty in the linear fittings around the crossover. Two major features emerge from Fig. 6(a) when

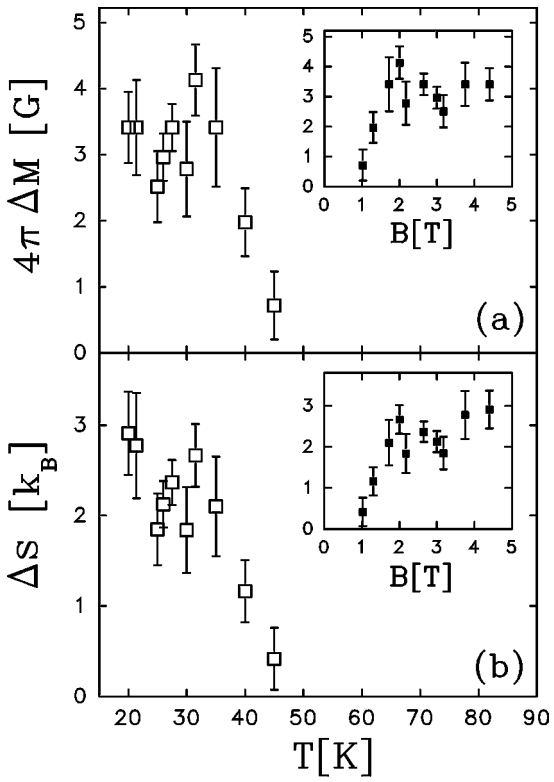

FIG. 6. (a) Magnitude of magnetization steps, derived from either H or T scans, as a function of temperature. Same data are plotted versus magnetic field in the inset. (b) Entropy variation per pancake as a function of temperature. Same data are plotted versus magnetic field in the inset.

one compares to most of the results in the literature on other compounds. First, the values of magnetization steps found at low T and high B are rather large in the present case. Second, they exhibit a rapid drop around a temperature which is very far from T_c. In Bi-2212, all the magnetic studies have reported ΔB ($=4\pi\Delta M$) values of a few tenths of gauss (typically 0.3 G), which are weakly temperature dependent before dropping to zero at T_c.[8,12–14] Although they continuously decrease as T is increased, values of the same order of magnitude were found in the first studies of YBCO.[2,3] On the other hand, significantly larger ΔB values (of a few gauss) have also been obtained in YBCO by dc magnetization measurements.[5]

In other respects, it can be noted that a direct comparison of Hg-1201 with Bi-2212 or YBCO is delicate because the magnetization steps in these compounds take place in very different regions of the H-t ($=T/T_c$) plane: very low fields for Bi-2212 or high temperatures staying close to T_c for YBCO, while one deals with both low temperatures ($T<T_c/2$) and large fields (of a few teslas) in Hg-1201.

Only local magnetic investigations in Bi-2212 have shown sharp discontinuities in vortex density, as expected for a first-order transition. All global magnetic measurements yielded rather broad, smooth steps in magnetization curves, even when the existence of a true first-order transition was clearly attested to by other techniques. Accordingly, the magnetization steps observed here in Hg-1201 can be related to an underlying first-order transition. On this assumption, the associated entropy variation can be evaluated via the

Clausius-Clapeyron relation, $\Delta S = -\Delta M(dH_i^*/dT)$, where H_i^* is the internal field at the transition. According to both the smallness of the magnetization as compared to H^* and the weak temperature dependence of H_{c1} in the region of interest,[26] one can safely identify, here, the derivative of H_i^* to that of $B^* \simeq H^*$. Most of the results in the literature are given in terms of entropy jump per pancake, $\Delta s = \Delta S \times d \times a_0^2$, where a_0 is the mean intervortex spacing:

$$\Delta s \simeq -d\Phi_0 \frac{\Delta M}{B^*} \frac{dB^*}{dT}. \tag{3.3}$$

The temperature and field dependences of Δs are plotted in Fig. 6(b). Like the steps in magnetization, these Δs values are larger than the greatest part of those found in YBCO, including direct determinations by calorimetric measurements[3–5,33] (values around 0.5 k_B). In Bi-2212, large Δs values of a few k_B have been reported,[11,12,14,26] but only close to T_c. The second peculiarity in Fig. 6(b) is the sudden vanishing of the entropy jump above 50 K. Even if the persistence of steplike features below our detection limit is not excluded at higher temperatures, there is undoubtedly a rapid, pronounced drop around $T = 45$ K.

As shown in the inset of Fig. 6(b), it is worth noticing that this end point can also be associated with a low-field boundary, located close to 1 T. In this respect, our results bear some resemblance to many results obtained on YBCO, in which any clear indication of a first-order transition is no longer detected below a certain field. A low-field boundary close to 1 T was indeed reported by Welp *et al.*[2] and Schilling *et al.*[3] in YBCO single crystals studied by SQUID magnetometry. Similar behaviors have also been observed in calorimetric measurements with limit field values equal to 1 T (Ref. 3 and 4) or 6 T.[5,33] Since these features correspond to temperatures very close to T_c in YBCO, the sample inhomogeneity was suspected to play a role in this behavior.[2,3] Nevertheless, such an influence can hardly be relevant to the present case of Hg-1201, because this limit point takes place at a temperature much below T_c. More likely, a boundary at low fields could be related to a pinning effect. As suggested in previous studies,[5,16,33] the vortex behavior can be strongly dominated by the presence of pinning centers up to a certain field value related to the defect density. Consequently, any first-order transition involving a well-ordered vortex state can be obtained only above a threshold field corresponding to the saturation of pinning centers.

IV. CONCLUSION

The occurrence of steps in magnetization curves, which can be related to a first-order transition, has been evidenced in Hg-1201. At the lowest temperatures (highest fields), these features take place in a fully reversible regime. At higher temperatures, the low-field side of the step lies in the irreversible regime. However, by using a careful recording procedure, one can get reliable estimates of the equilibrium magnetization in a part of the irreversible regime, allowing us to extend our estimates of the step height to high temperatures. Any thermodynamic signature of a phase transition abruptly disappears for fields lower than 1 T, similar to the behavior often observed in YBCO. Assuming an underlying first-order transition, the entropy changes inferred from the magnetization steps at low temperatures are found to be somewhat larger than most of the reported values in Bi-2212 and YBCO. Further experimental investigations, involving different techniques, are highly desirable to shed light on this last issue.

[1] R. Liang, D.A. Bonn, and W.N. Hardy, Phys. Rev. Lett. **76**, 835 (1996).

[2] U. Welp, J.A. Fendrich, K.W. Kwok, G.W. Crabtree, and B.W. Veal, Phys. Rev. Lett. **76**, 4809 (1996).

[3] A. Schilling, R.A. Fisher, N.E. Phillips, U. Welp, D. Dasgupta, W.K. Kwok, and G.W. Crabtree, Nature (London) **382**, 791 (1996).

[4] A. Schilling, R.A. Fisher, N.E. Phillips, U. Welp, W.K. Kwok, and G.W. Crabtree, Phys. Rev. Lett. **78**, 4833 (1997).

[5] A. Junod, M. Roulin, J.Y. Genoud, B. Revaz, A. Erb, and E. Walker, Physica C **275**, 245 (1997).

[6] M. Willemin, A. Schilling, H. Keller, C. Rossel, J. Hofer, U. Welp, W.K. Kwok, R.J. Olsson, and G.W. Crabtree, Phys. Rev. Lett. **81**, 4236 (1998).

[7] A. Schilling, R.A. Fisher, N.E. Phillips, U. Welp, W.K. Kwok, and G.W. Crabtree, Phys. Rev. B **58**, 11 157 (1998).

[8] E. Zeldov, D. Majer, M. Konczykowski, V.B. Geshkenbein, V.M. Vinokur, and H. Shtrikman, Nature (London) **375**, 373 (1995).

[9] Y. Yamaguchi, N. Aoki, F. Iga, and Y. Nishihara, Physica C **246**, 216 (1995).

[10] B. Revaz, G. Triscone, L. Fabrega, A. Junod, and J. Muller, Europhys. Lett. **33**, 701 (1996).

[11] T. Hanaguri, T. Tsuboi, A. Maeda, T. Nishizaki, N. Kobayashi, Y. Kotaka, J. Shimoyama, and K. Kishio, Physica C **256**, 111 (1996).

[12] N. Morozov, E. Zeldov, D. Majer, and M. Konczykowski, Phys. Rev. B **54**, R3784 (1996).

[13] S. Ooi, T. Shibauchi, and T. Tamegai, Physica C **302**, 339 (1998).

[14] K. Kadowaki and K. Kimura, Phys. Rev. B **57**, 11 674 (1998).

[15] T. Sasagawa, K. Kishio, Y. Togawa, J. Shimoyama, and K. Kitazawa, Phys. Rev. Lett. **80**, 4297 (1998).

[16] L. Fruchter, A. Aburto, and C. Pham-Phu, Phys. Rev. B **56**, R2936 (1997).

[17] T. Shibauchi, M. Sato, S. Ooi, and T. Tamegai, Phys. Rev. B **57**, R5622 (1998).

[18] M.J.W. Dodgson, V.B. Geshkenbein, H. Nordborg, and G. Blatter, Phys. Rev. Lett. **80**, 837 (1998).

[19] G. Le Bras, L. Fruchter, V. Vulcanescu, V. Viallet, A. Bertinotti, A. Forget, J. Hammann, J.-F. Marucco, and D. Colson, Physica C **271**, 205 (1996).

[20] J. Hofer, J. Karpinski, M. Willemin, G.I. Meijer, E.M. Kopnin, R. Molinski, H. Schwer, C. Rossel, and H. Keller, Physica C **297**, 103 (1998).

[21] D. Pelloquin, V. Hardy, A. Maignan, and B. Raveau, Physica C **273**, 205 (1997).

[22] G. Villard, A. Daignere, D. Pelloquin, and A. Maignan, Physica C **314**, 196 (1999).

[23] G. Villard, A. Daignere, A. Maignan, and A. Ruyter, J. Appl. Phys. **84**, 5080 (1998).
[24] J.R. Kirtley, K.A. Moler, G. Villard, and A. Maignan, Phys. Rev. Lett. **81**, 2140 (1998).
[25] E. Zeldov, A.I. Larkin, V.B. Geshkenbein, M. Konczykowski, D. Majer, B. Khaykovich, V.M. Vinokur, and H. Shtrikman, Phys. Rev. Lett. **73**, 1428 (1994).
[26] A.I.M. Rae, E.M. Forgan, and R.A. Doyle, Physica C **301**, 301 (1998).
[27] S.L. Lee, C.M. Aegerter, H. Keller, M. Willemin, B. Stäuble-Pümpin, E.M. Forgan, S.H. Lloyd, G. Blatter, R. Cubitt, T.W. Li, and P. Kes, Phys. Rev. B **55**, 5666 (1997).
[28] A. Houghton, R.A. Pelcovits, and A. Sudbo, Phys. Rev. B **40**, 6763 (1989).
[29] G. Blatter, M.V. Feigel'man, V.B. Geshkenbein, A.I. Larkin, and V.M. Vinokur, Rev. Mod. Phys. **66**, 1125 (1994).
[30] L.I. Glazman and A.E. Koshelev, Phys. Rev. B **43**, 2835 (1991).
[31] L.L. Daemen, L.N. Bulaevskii, M.P. Maley, and J.Y. Coulter, Phys. Rev. B **47**, 11 291 (1993).
[32] Equation (3.2) with $n=1$ corresponds to a T dependence of the form $B^* \propto (T_c - T)/T$, often reported in the literature (Refs. 8, 14, and 15).
[33] B. Revaz, A. Junod, and A. Erb, Phys. Rev. B **58**, 11 153 (1998). This study was performed on $DyBa_2Cu_3O_7$.